NASA/TP-2005-213164

Managing Lunar and Mars Mission Radiation Risks
Part I: Cancer Risks, Uncertainties, and Shielding Effectiveness

Francis A. Cucinotta
NASA Lyndon B. Johnson Space Center
Houston, Texas

Myung-Hee Y. Kim
Wyle Laboratories
Houston, Texas

Lei Ren
U.S.R.A., Division of Space Life Science Division
Houston, Texas

July 2005

THE NASA STI PROGRAM OFFICE . . . IN PROFILE

Since its founding, NASA has been dedicated to the advancement of aeronautics and space science. The NASA Scientific and Technical Information (STI) Program Office plays a key part in helping NASA maintain this important role.

The NASA STI Program Office is operated by Langley Research Center, the lead center for NASA's scientific and technical information. The NASA STI Program Office provides access to the NASA STI Database, the largest collection of aeronautical and space science STI in the world. The Program Office is also NASA's institutional mechanism for disseminating the results of its research and development activities. These results are published by NASA in the NASA STI Report Series, which includes the following report types:

- TECHNICAL PUBLICATION. Reports of completed research or a major significant phase of research that present the results of NASA programs and include extensive data or theoretical analysis. Includes compilations of significant scientific and technical data and information deemed to be of continuing reference value. NASA's counterpart of peer-reviewed formal professional papers but has less stringent limitations on manuscript length and extent of graphic presentations.

- TECHNICAL MEMORANDUM. Scientific and technical findings that are preliminary or of specialized interest, e.g., quick release reports, working papers, and bibliographies that contain minimal annotation. Does not contain extensive analysis.

- CONTRACTOR REPORT. Scientific and technical findings by NASA-sponsored contractors and grantees.

- CONFERENCE PUBLICATION. Collected papers from scientific and technical conferences, symposia, seminars, or other meetings sponsored or cosponsored by NASA.

- SPECIAL PUBLICATION. Scientific, technical, or historical information from NASA programs, projects, and mission, often concerned with subjects having substantial public interest.

- TECHNICAL TRANSLATION. English-language translations of foreign scientific and technical material pertinent to NASA's mission.

Specialized services that complement the STI Program Office's diverse offerings include creating custom thesauri, building customized databases, organizing and publishing research results . . . even providing videos.

For more information about the NASA STI Program Office, see the following:

- Access the NASA STI Program Home Page at http://www.sti.nasa.gov

- E-mail your question via the Internet to help@sti.nasa.gov

- Fax your question to the NASA Access Help Desk at (301) 621-0134

- Telephone the NASA Access Help Desk at (301) 621-0390

- Write to:
  NASA Access Help Desk
  NASA Center for AeroSpace Information
  7121 Standard
  Hanover, MD 21076-1320

NASA/TP-2005-213164

Managing Lunar and Mars Mission Radiation Risks
Part I: Cancer Risks, Uncertainties, and Shielding Effectiveness

Francis A. Cucinotta
NASA Lyndon B. Johnson Space Center
Houston, Texas

Myung-Hee Y. Kim
Wyle Laboratories
Houston, Texas

Lei Ren
U.S.R.A., Division of Space Life Science Division
Houston, Texas

July 2005

Contents

Figures

Glossary

AGS	Alternating Gradient Synchrotron
ALARA	as low as reasonably achievable
BEIR	biological effect of ionizing radiation
BRYNTRN	baryon transport code
CAMERA	computerized anatomical man model
CEV	Crew Exploration Vehicle
CI	confidence intervals
CL	confidence level
CNS	central nervous system
DDREF	dose and dose-rate reduction factor
EAR	excess additive risk, Sv^{-1}
ELR	excess lifetime risk
ERR	excess relative risk, $Sv^{-1} \, yr^{-1}$
F	tissue-weighted fluence, no. ions/cm^2
GCR	galactic cosmic rays
GSD	geometric standard deviation
HZE	high-energy and charge
HZETRN	high charge and energy transport
ICRP	International Commission on Radiological Protection
ISS	International Space Station
LEO	low Earth orbit
LET	linear energy transfer
LLE	loss of life-expectancy, yr
LLER	loss of life-expectancy amongst exposure-induced deaths, yr
LSS	life-span study of the Japanese atomic-bomb survivors
$M_c(a)$	gender and age-specific cancer mortality rate in the U.S. population
NAS	National Academy of Sciences
NCRP	National Council on Radiation Protection and Measurements
NRC	National Research Council
NSRL	NASA Space Radiation Laboratory
PDF	probability distribution function
Q	quality factor
Q(L)	quality factor as a function of linear energy transfer
QMSFRG	quantum multiple scattering fragmentation
RBE	relative biological effectiveness

RBE~max~	maximum relative biological effectiveness that assumes the dose is linear at low doses or dose-rates
REID	risk of exposure-induced death
S.D.	standard deviations
SEER	surveillance, epidemiology, and end results
SHE	Syrian hamster embryo
SOBP	spread out Bragg peak
SPE	solar particle event
SSA	Social Security Administration
TEPC	tissue equivalent proportional counter
x_α	quantiles (random variables) associated with factor α

Abstract

We discuss calculations of probability distribution functions (PDFs) representing uncertainties in projecting fatal cancer risk from galactic cosmic rays (GCR) and solar particle events (SPEs). The PDFs are used in significance tests of the effectiveness of potential radiation shielding approaches. Using Monte-Carlo techniques, we propagate uncertainties in risk coefficients determined from epidemiology data, dose and dose-rate reduction factors, quality factors, and physics models of radiation environments to formulate cancer risk PDFs. Competing mortality risks and functional correlations in radiation quality factor uncertainties are treated in the calculations. We show that the cancer risk uncertainty, which is defined as the ratio of the 95% confidence level (CL) to the point estimate, is about four-fold for lunar and Mars mission risk projections. For short-stay (<180 d) lunar missions, SPEs present the most significant risk, but one that is mitigated effectively by shielding, especially for carbon composites structures with high hydrogen content. In contrast, for long-duration (>180 d) lunar or Mars missions, GCR risks may exceed radiation risk limits, with 95% CLs exceeding 10% fatal risk for males and females on a Mars mission. Shielding materials are marginally effective in reducing GCR cancer risks because of the penetrating nature of GCR and secondary radiation produced in tissue by relativistic particles. Currently, based on a significance test that accounts for radiobiology uncertainties in GCR risk projection, polyethylene or carbon composite shielding cannot be shown to significantly reduce risk compared to aluminum shielding. We therefore conclude that improving knowledge of space radiobiology to narrow uncertainties that lead to wide PDFs is the most effective approach to ensure radiation protection goals are met for space exploration.

1. Introduction

This is the first in a three-part series addressing issues related to managing radiation risks for lunar and Mars missions that will focus on preflight safety preparations, including risk projections and shielding effectiveness. The first part addresses cancer risks, the second part acute radiation risks from solar particle events (SPEs), and the third part non-cancer risks including damage to the central nervous system (CNS). Exposures to astronauts from galactic cosmic rays (GCR)—which are made up of high-energy protons and high-energy and charge (HZE) nuclei, and SPEs, which are comprised largely of low- to medium-energy protons—are important safety concerns for space exploration. Radiation risks include carcinogenesis, degenerative tissue effects such as cataracts (Cucinotta *et al*., 2001a) or heart diseases (Preston *et al*., 2003, Howe *et al.,* 2004, Yang and Ainsworth, 1982), and acute radiation syndromes (NCRP, 2000). Other risks, such as damage to the CNS, are a concern for HZE nuclei (NAS, 1996). In the past, career radiation limits were based on fatal cancer risks. For low Earth orbit (LEO) programs, an excess fatal risk of 3% is used as criteria for dose limits, which are applied using age- and gender-specific dose to risk conversion factors. Although standards for lunar missions are under review at this time, it is expected that cancer risks will be the major component of radiation limits until knowledge on chronic non-cancer risks from radiation are more firmly established.

Radiation risk projection models serve several roles; these roles include setting dose-to-risk conversion factors needed to define dose limits, projecting mission risks, and evaluating the effectiveness of shielding or other countermeasures. For mission planning and operations, NASA uses the model recommended in the NCRP Report No. 132 for estimating cancer risks from space (NCRP, 2000). This model, which is similar to approaches described by other radiation risk assessment committees or in the scientific literature, employs a life-table formalism, epidemiological assessments of excess risk in exposed cohorts such as the atomic-bomb survivors, and estimates of dose and dose-rate reduction factors (DDREFs) and linear energy transfer (LET)-dependent

radiation quality factors. Recently, NASA recognized that projecting uncertainties in cancer risk estimates along with point estimates should be a requirement for ensuring mission safety, because point estimates alone have limited value when the uncertainties in the factors that enter into risk calculations are large. Estimates of 95% confidence intervals (CI) for various radiation protection scenarios are meaningful additions to the traditional point estimates, and can be used to explore the value of mitigation approaches and of research that could narrow the various factors that enter into risk calculations. Designing space missions with acceptable levels of cancer risks can take several pathways. Because of the penetrating nature of the GCR and the buildup of secondary radiation in tissue behind practical amounts of all materials, we argued previously (Cucinotta *et al.*, 2001b, 2002, 2004) that improving knowledge of biological effects to narrow confidence intervals is the most effective approach to achieve radiation safety goals.

Uncertainties for low-LET radiation, such as gamma-rays, have been reviewed several times in recent years, and indicate that the major uncertainty is the extrapolation of cancer effects data from high to low doses and dose-rates (NCRP, 1997; BEIR, 1994). Other uncertainties include the transfer of risk across populations and sources of error in epidemiology data including dosimetry, bias, and statistical limitations. For low-LET radiation, probability distribution functions (PDFs) were described previously (NCRP, 1997). In estimating cancer risks for space radiation, additional uncertainties occur related to estimating the biological effectiveness of protons and heavy ions, and to predicting LET spectra at tissue sites (Cucinotta *et al.*, 2001b). The limited understanding of heavy ion radiobiology has been estimated to be the largest contributor to the uncertainty for space radiation effects (NAS, 1996), and radiation quality factors were found to contribute the major portion of the uncertainties in a previous study (Cucinotta *et al.*, 2001b).

In this report, we discuss modifications to our methodology for projecting cancer risk probability distributions for space missions and apply the model to several space exploration mission scenarios, including the evaluation of potential shielding approaches: First, in our previous work, we had assumed the normal approximation for summing the additive contributions of many radiation components at tissue sites behind spacecraft shielding. The fluence weighted variance for each GCR charge and energy group was summed using the square root of the sum of the squares to estimate the standard deviation and confidence intervals. In this work, we have used direct sampling over organ-weighted LET distributions for the estimation of the 95% CIs, and shown that a log-normal distribution results from the analysis. A second modification is related to the uncertainties in the radiation quality factors. Previously, we had considered the range of experimental data for appropriate endpoints to develop a subjective PDF for the quality factor. In this paper, we treat the quality factor, *Q(L)*, and its uncertainties as a functional relationship, which recognizes that values of *Q(L)* at different LETs are in fact correlated by underlying biophysical processes. The final improvement made here is to accumulate Monte-Carlo trials directly from the double-detriment life-table rather than the cancer mortality rate. The life-table approach is used because, in our previous estimates of cancer risk for the Mars mission (Cucinotta *et al.*, 2001b), the upper level of the 95% CI exceeded 10% mortality risk, and we expect that competing causes of death may significantly compress the higher values in the distribution. By sampling directly from a life-table, we are also able to study a probability distribution for reduced life-expectancy from space radiation exposure. Our risk estimates are based on the quantity risk of exposure-induced death (REID) rather than excess lifetime risk (ELR) to properly account for competing risks (Vaeth and Pierce, 1990) and to enable easier comparisons to other space mission risks.

Shielding is one approach that can be considered for mitigating radiation risks. Theoretical and computational efforts in the 1980's and 1990's provided the basic understanding

needed to design effective shielding approaches (Wilson *et al.*, 1991, 1995, Cucinotta *et al.*, 1998a). Materials of low atomic mass, especially hydrogen, are expected to be optimal as radiation shields because they reduce the occurrence of secondary particles (neutrons, protons, and other recoils) and are more effective per unit mass of material in slowing or stopping ions in atomic collisions and fragmenting HZE ions. However, because relativistic ions in the GCR are not appreciably slowed by appreciable amounts of any material and are the largest inducer of secondary radiation produced in tissues, the role of shielding material selection for GCR is not clear. We demonstrate here that shielding materials cannot be shown to have an important role in reducing GCR risks because of their poor attenuation properties in any material combined with large risk model uncertainties. In contrast, exposures to SPEs are effectively mitigated by most shielding materials, and there is a substantial reduction in mass that occurs when lower mass materials are selected for spacecraft structures.

2. Life-Table Methodology

We use the double detriment life-table to estimate radiation cancer mortality risks. In this approach, the age-specific mortality of a population is followed over its entire lifespan with competing risks from radiation and all other causes of death described (Bunger *et al.*, 1981). For a homogeneous population receiving an effective dose E at age a_E, the probability of dying in the age interval from a to $a+1$ is described by the background mortality rate for all causes of death, $M(a)$, and the radiation cancer mortality rate, $m(E,a_E,a)$, as

$$q(E,a_E,a) \;=\; \frac{M(a)+m(E,a_E,a)}{1+\dfrac{1}{2}[M(a)+m(E,a_E,a)]} \tag{1}$$

The survival probability to live to age a following an exposure E at age a_E is

$$S(E,a_E,a) \;=\; \prod_{u=a_E}^{a-1}[1-q(E,a_E,u)] \tag{2}$$

ELR, which is the increased probability that an exposed individual will die from cancer, is defined by the difference in the conditional survival probabilities for the exposed and unexposed groups as

$$ELR \;=\; \sum_{a=a_E}^{\infty}[M(a)+m(E,a_E,a)]S(E,a_E,a) - \sum_{a=a_E}^{\infty} M(a)S(0,a_E,a) \tag{3}$$

We use a finite cutoff of 101 years for the upper limit in Eq.(3) and expressions below. Although a minimum latency time of 10 years is often used for low-LET radiation (NCRP, 2000), we will consider alternative assumptions for high-LET radiation. *REID* is the lifetime risk that an individual in the population will die from a cancer caused by his or her radiation exposure; it is defined by

$$REID \quad = \quad \sum_{a=a_E}^{\infty} m(E,a_E,a)S(E,a_E,a) \qquad (4)$$

In general, the value of REID exceeds that of ELR by about 10–20%. Vaeth and Pierce (1990) have discussed special cases where ELR is ill-defined and suggested that REID is the preferred quantity for radiation protection. The loss of life-expectancy amongst exposure-induced deaths, denoted here as *LLER*, is defined (Vaeth and Pierce, 1990) as

$$LLER \quad = \quad \frac{LLE}{REID}, \qquad (5)$$

where the average loss of life-expectancy, *LLE,* in the population is defined by

$$LLE \quad = \sum_{a=a_E}^{\infty} S(0,a_E,a) - \sum_{a=a_E}^{\infty} S(E,a_E,a). \qquad (6)$$

2.1 Radiation carcinogenesis mortality rate

For projecting lifetime cancer fatality risks, an age- and gender-dependent mortality rate per unit dose, estimated for acute gamma-ray exposures, is multiplied by the radiation quality factor and reduced by the DDREF (NCRP, 2000); additivity of effects of each component in a radiation field is assumed. Radiation mortality rates are largely modeled using the Japanese atomic-bomb survivor data. For transferring risks from the Japanese to the U.S. population, two models are often considered. The multiplicative transfer model assumes radiation risks are proportional to spontaneous or background cancer risks, and the additive transfer model assumes radiation acts independently of other cancer risks. However, the NCRP recommends (NCRP, 2000) a mixture model with fractional contributions from the multiplicative risk model or additive risk model. The radiation mortality rate is written as

$$m(E,a_E,a) \quad = \quad [\nu ERR(a_E,a)M_c(a)+(1-\nu)EAR(a_E,a)]\frac{\sum_L Q(L)F(L)L}{DDREF} \qquad (7)$$

where *ERR* and *EAR* are the excess relative risk and excess additive risk per Sievert, respectively, $M_c(a)$ is the gender- and age-specific cancer mortality rate in the U.S. population, *F* is the tissue-weighted fluence, *L* is the LET, and *Q* is the quality factor. Also in Eq. (7), ν is the fractional division between the assumption of the multiplicative and additive risk transfer models. For solid cancer, it is assumed that $\nu=1/2$; and for leukemia, it is assumed that $\nu=0$.

3. Uncertainties in the Projection Model

Equation (7) consists of a product of several factors: the *ERR* or *EAR*, the background cancer rates, M_c, the effective dose represented by the physical dose, *FL*, times the radiation quality factor, *Q(L)*, and the *DDREF*. The limiting behavior of the addition of many random variables is well known as the normal distribution. In contrast, the limiting behavior of the multiplication of many random factors will be a log-normal distribution. Equation (7) assumes each multiplicative factor is independent. This assumption may not be strictly valid because of

possible correlations between factors or non-additivity of different radiation components, since cells will be traversed by multiple particles and delta-rays produced by ions passing through adjacent cell layers (Cucinotta *et al.*, 1998b). We next consider estimates of the range of values and associated PDFs for each of these factors. Because the risk for longer duration missions exceeds a few percent, the upper 95% CI may exceed 10%. In such cases, the sampling of rates is insufficient, and the expression for the REID given by Eq. (4) must be used because of competing risks from other causes of death that will reduce the likelihood of very large radiation risks. Therefore, in the sampling approaches described below, trials are accumulated for the REID rather than the mortality rate. A criteria used in our approach for formulating PDFs for various factors is to ensure the PDFs are peaked at the values recommended by the NCRP (NCRP, 2000), such as the DDREF and Q, or in the current physics models of radiation environments and transport used in mission projections or spacecraft designs. We next discuss the uncertainties in the projection model.

3.1 Uncertainties in low linear energy transfer epidemiology data

For sampling purposes, the low-LET mortality rate per Sievert, m_L, is written

$$m_l(E,a_x,a) \quad = \quad \frac{m_0(E,a_x,a)}{DDREF} \frac{x_D x_s x_T x_B}{x_{Dr}}, \tag{8}$$

where m_0 is the baseline mortality rate per Sievert (see Eq. (7)) and the x_α are quantiles (random variables) whose values are sampled from an associated PDF, $P(x_\alpha)$. Note that the DDREF applies only to the solid cancer risk and not to the leukemia risk under the stated assumptions. The NCRP Report 126 (NCRP, 1997) defines the following subjective PDFs, $P(x_\alpha)$, for each factor that contributes to the low LET-risk projection:

1. $P_{dosimetry}$ represents random and systematic errors in the estimation of the doses received by atomic-bomb blast survivors. It is assumed as a normally distributed PDF for bias correction of random and systematic errors in the dosimetry (DS86) with mean 0.84 and standard deviation 0.11;
2. $P_{statistical}$ represents the distribution in uncertainty in the risk coefficient r_0. It is assumed as a normally distributed PDF with a mean of 1 and a standard deviation of 0.15;
3. P_{bias} represents any bias resulting for over- or under-reporting cancer deaths. P_{bias} is assumed as a normal distribution with a most probable value of 1.1 and a 90% CI from 1.02 to 1.18 corresponding to a standard deviation of 0.05;
4. $P_{transfer}$ represents the uncertainty in the transfer of cancer risk following radiation exposure from the Japanese population to the U.S. population. Both additive and relative risks models were considered by the NCRP 126 report (NCRP, 1997) in assessing the uncertainties in such transfer. $P_{transfer}$ is log-normal with a mean of 1 and a standard deviation of 0.26 (GSD=1.3);
5. P_{Dr} represents the uncertainty in the knowledge of the extrapolation of risks to low dose and dose-rates embodied in the DDREF. The NCRP assumed P_{Dr} to be a truncated triangle distribution starting at 1 and ending at 5 with a peak at 2 and with a relative value of ¼ or ½ at 1 or 5, respectively, compared to the peak values for the DDREF at 2. This PDF is used to scale the low-LET risk coefficient (mortality rates) in our estimates for space radiation.

The NCRP also considered a PDF for bias correction in projection of cancer risks over a lifetime. It is ignored herein, however, because the astronaut population is generally over age 30 y and the Japanese data are now complete for these ages. We also ignore the assumed "unknown uncertainties" from the NCRP 126 report (NCRP, 1997).

3.2 Uncertainties due to dose-rate and protraction effects for ions

For low dose-rate and protracted proton and HZE radiation exposure of more than a few months, new biological factors may influence risk assessments including redistribution in the cell cycle, repopulation, or promotional effects, especially when particle fluences are large enough to lead to multiple hits of target cells or surrounding cells and tissue environments. Also, not only are there no human data for protons and HZE ions, there are very little experimental data at low dose-rates for these particles. Confidence in using radio-epidemiological data for acute (A-bomb survivors) or fractionated (patients) data is decreased when applied to protracted exposure. Burns *et al*. (1994) found split doses of argon ions separated by a few hours up to one day increased the risk of skin cancer in rats. Alpen *et al*. (1994) found using seven 2-week fractions of 0.07 Gy of iron increased risk to 50% compared to a single acute dose of 0.4 Gy for Harderian gland tumors in mice. A study of chromosomal aberrations in human lymphocytes (George *et al*., 2002 for acute and low dose-rates (0.08 Gy/hr) with 250 MeV protons showed less sparring than found for gamma-rays. The Skyhook study of Ainsworth (1986) considered life-shortening in mice comparing single acute with weekly fractions of several ions; however, the results were unclear with regards to any increase or decrease in risk.

For gamma-rays and neutrons, a number of studies for cancer induction or life-shortening in mice exist, showing sparring effects for gamma-rays and that neutron effects may be increased due to protraction under certain conditions in some tissues (Ullrich, 1984; NCRP, 1990). Important questions related to the differences in lifespan, cell turnover rates, or mechanisms of initiation or promotion in humans and mice make estimates of the effects of protraction on risk difficult. If protraction effects do increase the risk from high-LET radiation, such effects would be more important for a Mars mission than for the shorter lunar missions. In space, each cell will be traversed about every two to three days by a proton or delta-ray produced by ions in adjacent cells, and with a decreasing frequency from weeks to months as the charge of the HZE nuclei increases (Cucinotta *et al*., 1998b). Studies of mixed fields of protons and HZE ions are needed to understand uncertainties in dose-rate and protraction effects from space radiation. Uncertainties related to radiation quality, dose-rate, and protraction could lead to correlations that will be difficult to describe when based on limited experimental data. Methods to treat correlation effects will be needed when data on protraction effects become available.

3.3 Radiation quality and latency or temporal patterns of risk

An additional radiation quality uncertainty is introduced by the scaling assumption used in Eq. (7) because the time dependence for low- and high-LET radiation is assumed to be identical. Data on tumors or genomic instability in mice with neutrons (Ullrich, 1984; Ullrich and Ponnaiva, 1998; NCRP, 1990) and the studies of rat or mammary carcinogenesis with HZE nuclei (Burns, *et al.*, 1994; Dicello *et al.*, 2004) suggest that the latency time is appreciably reduced for high-LET radiation compared to low LET-radiation. Sparse data are available to estimate the impact of these differences on uncertainties. A radiation quality-dependent latency is more important in the additive transfer model than in the multiplicative transfer model, especially at younger ages of exposure. Also, for high-LET radiation, a constant ERR with time after exposure assumption, following an early latency period, is difficult to prove based on current animal carcinogenesis data. We ignore these uncertainties; however, we replace the 10-year minima latency assumption made for low LET by the step-in latency model (Pierce *et al*., 1996) used for the leukemia risk. The effects of these assumptions will need to be addressed when data and knowledge on underlying mechanisms become available.

3.4 Uncertainties in quality factors

Radiation quality factors represent the largest uncertainty in estimating space radiation cancer risks. Past reviews on the relative biological effectiveness of high-LET radiation include ICRP Report 40 (1986), NCRP Report 104 (1990), and more recently ICRP Report 92 (2003). The practice, followed by committees, of assigning radiation quality factors is to consider an average of the relative biological effectiveness (RBE) factors at low doses (RBE_{max}) for the most relevant experimental endpoints. Uncertainties in assignment of RBEs for protons and heavy ions arise for several reasons including sparseness of data for tumorigenesis in animal models or surrogate tissue or cellular endpoints, variability in reference radiation and doses and dose-rates employed, and lack of data over the LET range of interest. Also, linearity at low dose or dose-rates for the reference radiation or ions is frequently not sufficiently established in experiments. Statistical limitations often hinder studies at the low dose-rates of interest for space radiation protection. For high-LET radiation, a turnover or bending found in the dose response for tumor induction and neoplastic transformation is observed at moderate doses, presenting further uncertainties in estimating the effectiveness of high-LET radiation at low dose-rates.

Figure 1 shows representative examples of the ratio of RBE_{max} to Q for mouse tumors, cell transformation or mutations, or cytogenetic endpoints. The ratio is often two- to three-fold higher or lower than unity, indicating the expected deviation from Q in available data. **Table 1** shows LET values at the maximum RBE found in past studies selected from experiments where >5 ions were employed. Large deviations from the Q peak at 100 keV/μm are observed in these experiments with a range from about 50 to 190 keV/μm for the peak. These data are largely from the facilities at Berkeley, Calif., Darmstadt, Germany, Chiba, Japan, and the Alternating Gradient Synchrotron (AGS), Brookhaven National Laboratory, Upton, NY. The number of past studies
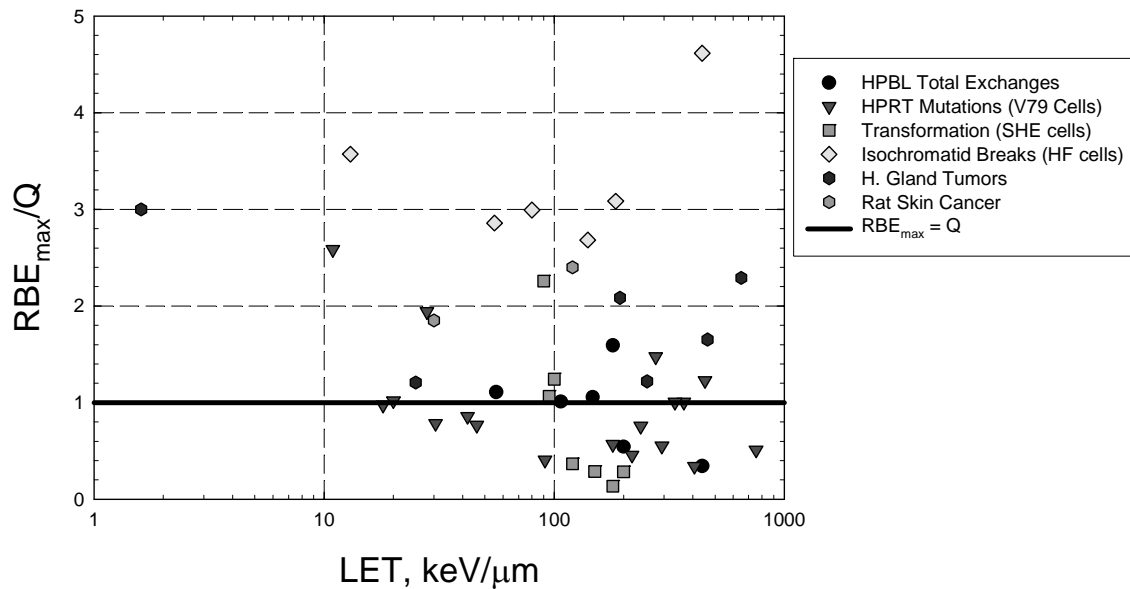
Figure 1. Comparison of ratio of RBE_{max} to Q for several endpoints found with proton, alpha particle, and heavy ion irradiations (reference experiments listed in Table 1).

Table 1. Approximate LET where maximum RBE was found in biological experiments

Biological system	Endpoint	LET at peak RBE, keV/μm	LET range (no. of ions studied)	Reference
Human TK6 lymphoblasts cells	TK mutants	60	32–190 (6)	Kronenberg (1994)
Human TK6 lymphoblasts cells	HPRT mutants	60	32–190 (6)	Kronenberg (1994)
Human lung fibroblasts	HPRT mutants	90	20–470 (9)	Cox and Masson (1979)
Human skin fibroblasts	HPRT mutants	150	25–920 (7)	Tsuoboi *et al.* (1992)
V79 Chinese hamster cells	HPRT mutants	90	10–2000 (16)	Kiefer *et al.* (1994); Belli *et al.* (1993)
Caenorhabditis elegans	Recessive lethal mutations	190	0.55–1110 (14)	Nelson *et al.* (1989)
Human lymphocyte cells	Chromosomal exchanges	147	0.4–1000 (10)	George *et al.* (2003)
Human fibroblast cells	Chromatid breaks	80-185	13–440 (6)	Kawata *et al.* (2001)
C3H10T1/2 mouse cells	Transformation	140	10–2000 (10)	Yang *et al.* (1989)
C3H10T1/2 mouse cells	Transformation	90	20–200 (10)	Miller *et al.* (1995)
Syrian hamster embryo (SHE) cells	Transformation	90	20–200 (8)	Martin *et al.* (1995)
Mouse (B6CF$_1$)	H. gland tumors	185*	2–650 (6)	Fry *et al.* (1985)
Mouse (B6CF$_1$)	H. gland Tumors	193	0.4–1000 (7)	Alpen *et al.* (1993)
Mouse (CB6F$_1$)	Days life lost	52*	50–500 (6)	Ainsworth (1986)

*Track-segment or spread out Bragg peak (SOBP) irradiations.

and endpoints used are limited if viewed as surrogate endpoints for human carcinogenesis. Additional data for more appropriate endpoints should become available in the next few years at the NASA Space Radiation Laboratory (NSRL). Track structure models suggest that each ion species would have distinct RBE curves of similar shape, but with curves for lower charge ions peaking at a lower LET than higher charged ions (Katz *et al.*, 1971; Cucinotta *et al.*, 1996; Nikjoo *et al.*, 1999). Furthermore, above about 1 MeV/u lower charged ions have a higher biological effectiveness than higher charged ions of identical LET. Based on track structure models, we expect that data sets that consider only a few ions are insufficient for defining the radiation quality dependence of *Q*. LET response curves also are predicted to depend on the target size (e.g., for gene or chromosome region) and intrinsic radiation sensitivity, which includes the competition with cell death. These factors likely vary between tissues.

To account for uncertainties in quality factors, we introduce a trial function that has a shape guided by both experimental data and biophysical models, and sample from distributions of parameters that enter into the functional form. The $Q(L)$ trial function is defined as

$$Q_{trial}(L) \;=\; \begin{cases} 1 & L < L_0 \\ AL - B & L_0 \leq L < L_m \\ C / L^p & L \geq L_m \end{cases} \tag{9}$$

We sample values of L_0, L_m, p, and the maximum value $Q_m(L_m)$ from PDFs described below. Using Eq. (9), we can solve for values of the constants A, B, and C. Often-discussed issues on the definition of $Q(L)$, as embodied in Eq. (9), are the value of slope p that controls the decrease in $Q(L)$ above a maximum, the maximum value of $Q(L)$, the LET where the maximum occurs, L_m, and the minimum LET where $Q(L)$ rises above unity, L_0. We note the ICRP-60 Q-function corresponds to L_0=10 keV/µm, L_m=100 keV/µm, $p = ½$, and Q_m=30 such that A=0.32, B=2.2, C=300, and the ICRP-26 Q-function, L_0=3.5 keV/µm, L_m=172.5 keV/µm, p=0, and Q_m=20.

The parameter samplings are based on the following assumptions for PDFs:

a. L_0: equal probability between 5 and 10 keV/µm, and decreasing to zero at 1 keV/µm or above 15 keV/µm.
b. L_m: equal probability for LET values between 75 and 150 keV/µm, and decreasing to zero at 50 keV/µm or above 250 keV/µm.
c. p: equal probability between p=1/2 and 1, and decreasing to zero at p<0 or p>2.
d. Q_m: log-normal distribution with mean value of 30 and geometric standard deviation (GSD) of 1.8.

Figure 2 shows examples of trial $Q(L)$ functions that contribute in the sampling procedures, and **Figure 3** shows the resulting average $Q(L)$ and 95% CI after 20,000 trials. The resulting range is smaller than in our previous report (Cucinotta *et al.*, 2001b); however, it should be a reasonable estimate when the effects of dose protraction are not included in the uncertainty analysis.
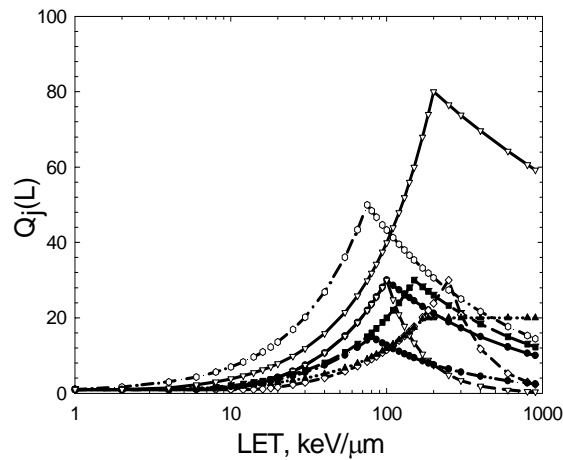

Figure 2. Examples of trial quality factor functions used in uncertainty calculations. A distinct curve is generated for each trial.
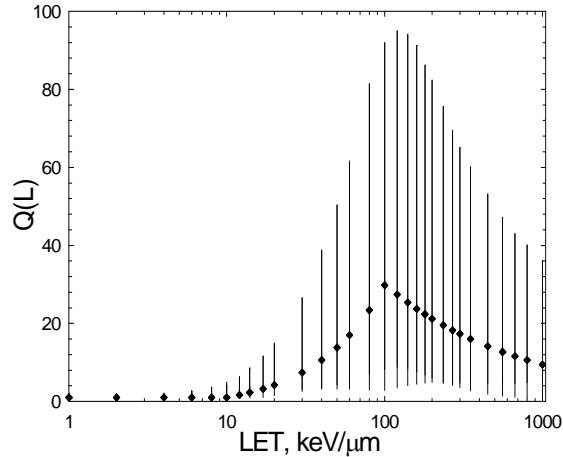
Figure 3. Average quality factor (circles) and 95% CI vs. LET from Monte-Carlo sampling over trial function of Eq. (9).

3.5 Uncertainties in physics: environments and transport codes

Space dosimetry and radiation transport codes have been studied extensively in the past and, although there are no major scientific questions that lead to errors in the assessment of space radiation environments, there are uncertainties due to limitations in dosimetry flown on past space missions. For application of computational models, the level of detail used in transport code comparisons is often limited, with common simplifications including the use of an aluminum equivalent shielding approximation, simplified geometries, and no description of orientation effects. Approaches to assess the errors in space dosimetry include inter-comparison of different dosimetry on the same missions as well as inter-comparison of results of space radiation transport models. Although statistical errors in the assessment of physical doses are quite small (<5%), inter-comparisons between laboratories have shown differences on the order of 10% for absorbed dose (Badhwar, 1997). Comparisons of transport calculations to measurements of LET spectra or dose equivalent should consider response functions of different detector types to charged particles or neutrons (Nikjoo *et al*., 2002). Commonly used detectors are tissue equivalent proportional counters (TEPCs), silicon detectors, and CR-39 plastic track detectors. However, good agreement has been found in the limited number of comparisons that have been made (e.g., Badhwar and Cucinotta, 2000; Kim *et al*., 2003; Shinn *et al*., 1998), especially when detector response functions are represented in the comparisons.

Models of the GCR environment rely on the large number of spaceflight and balloon measurements that have been made, and apply the diffusion theory of Parker (1965) to describe the modulation of the GCR over the solar cycle. The root mean square error for GCR environmental models is less than 10% for the major GCR elements and less than 15% for most minor elements (Badhwar and O'Neill, 1994a; Badhwar *et al*., 1994b; O'Neill, 2005). The isotopic composition of the GCR is also represented in transport codes (Cucinotta *et al*., 2003) used in risk calculations. SPE spectra vary from event to event, and no method is available to predict the fluence, energy spectra, or dose-rates of a future event. In this report, we discuss calculations for the large SPE of August 1972; risk assessment approaches to SPEs for acute risks will be considered in a future report. Transport codes rely on databases for nuclear interaction cross sections, including inclusive single differential in energy or total fragment production cross sections for

projectile fragments and double differential in energy and angle for lighter mass secondaries (neutrons, hydrogen and helium ions, and mesons). Cross-section data are sparse for some projection-target combinations and in the number of energies, especially above 1,000 MeV/u. Three-dimensional aspects of transport from angular scattering, a small correction for high-energy ions, are expected to be an important correction for neutrons and other light mass ions. Computer codes that use multi-group methods or Monte-Carlo simulations to describe angular effects on neutron transport have been developed for GCR shielding applications. The Monte-Carlo codes are limited by the computational times needed to describe spacecraft with thousands of parts, and the multi-group methods are limited by the ability to describe complex geometries. However, because flight measurements and the results of the HZETRN code (Wilson *et al.*, 1995) using the Badhwar-O'Neill GCR input spectra (Badhwar and O'Neill, 1994a) and the quantum multiple scattering fragmentation (QMSFRG) nuclear interaction database (Cucinotta *et al.*, 2003) are in good agreement, it is unclear whether such developments will have an important impact on risk assessment.

Differences between transport models and flight dosimetry that account for the detectors' response to different radiation components are generally small with absolute differences within 10% for the GCR dose and 20% for the GCR dose equivalent (Badhwar, 1997; Badhwar and Cucinotta, 2000 Cucinotta *et al.*; 2000; Cucinotta *et al.*, 2003). Measurements of dose or dose-equivalent may not provide sufficient information on possible errors in predicting LET spectra because compensating errors can occur. Also, neutron spectra are difficult to assess within complicated spacecraft and tissue geometries. In particular, measurements or calculations of neutron spectra are expected to lead to uncertainties in LET spectra in the LET range from about 30 to 300 keV/μm where recoil nuclei deposit the majority of the energy. Neutrons also cause a low-LET gamma-ray component that is often ignored in calculations. Larger errors are expected at higher LET values, where stopping nuclei dominate, and may be difficult to define due to local tissue variations. We expect uncertainties to be larger at high-LET values, where the role of local target recoils and stopping GCR primaries is difficult to describe.

The PDFs for the uncertainties in LET spectra should ensure that the resulting dose equivalent is consistent with transport code comparisons to past spaceflight measurements for GCR. A quantile, x_L, associated with a normal distribution, $P_F(x_F=F/F_0)$, is used with a standard error that increases with LET to represent the higher uncertainties expected for prediction of neutron effects and difficulty in precisely defining stopping ions in complex geometries. The PDF is given a median of x_{0F}=0.65 to ensure that the resulting dose equivalent is in agreement with values from the prior comparison between transport codes and flight measurements cited above. Standard deviations for different LET regions are given in **Table 2**.

Table 2. Standard deviations (S.D.) for uncertainties in model LET spectra for several LET regions

LET Interval	S.D. for dF/dL
<30 keV/μm	1.0
30–300 keV/μm	2.0
>300 keV/μm	2.5

Figure 4 and **Figure 5** illustrate the errors assigned to environmental and physical factors in evaluating LET spectra at tissue sites.
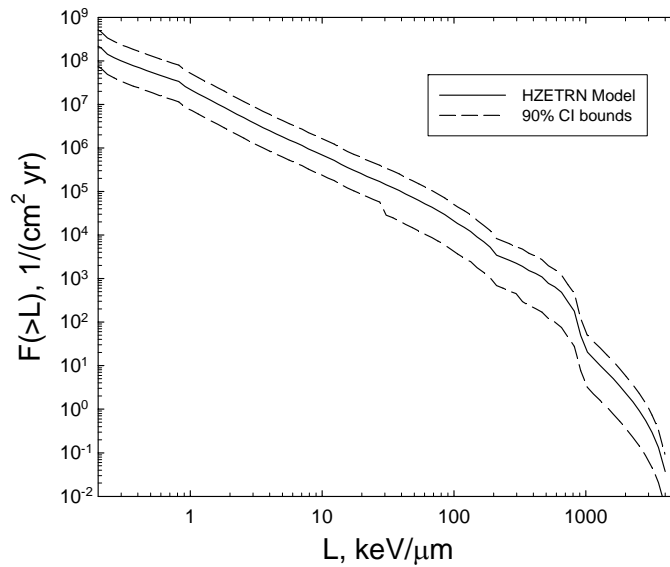
Figure 4. Calculation of tissue-weighted integral LET spectra and 90% CI for space environmental and transport uncertainties for 20 g/cm^2 aluminum shield for one year in deep space.
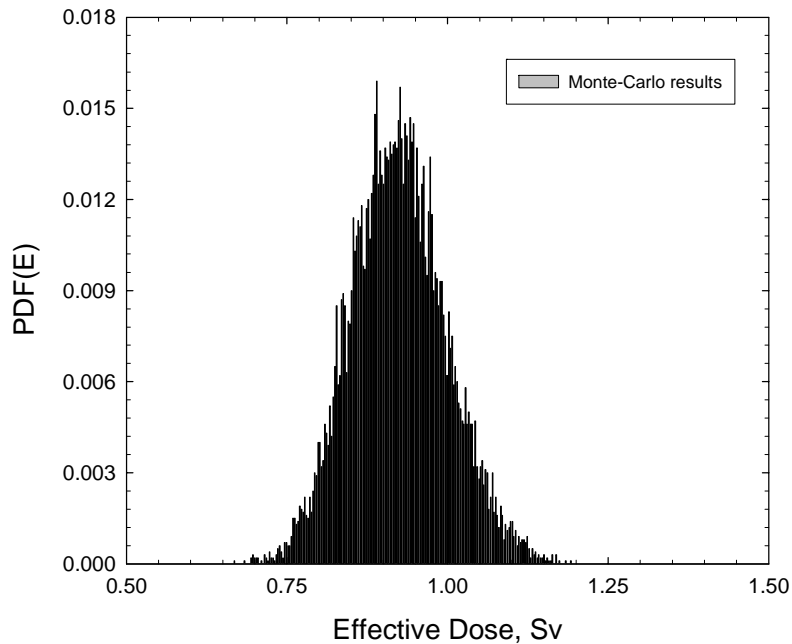

Figure 5. PDF for GCR effective dose for 20 g/cm^2 aluminum shield for 600-d Mars swingby mission. The point estimate is 0.86 Sv, and the 95% CI for uncertainties in LET distribution at tissue sites is [0.78, 1.08] Sv. Only uncertainties in physics are included.

3.6 Life-tables and population cancer rates

Although radiation risk calculations are based on population data, they are used to estimate risks for individuals. While population data reflect gender differences, these data also change with calendar year and are often used for projections far into the future. For the astronaut population, the appropriateness of using the U.S. average population can be questioned because the so-called "healthy worker" effect is expected for astronauts. In the average U.S. population, females have a longer lifespan than males, partially due to the overall lower risk of cancer. The formalism of Eq. (1) through Eq. (7) shows that two counteracting effects arise when we attempt to determine whether the use of population rates representative of a healthier population as compared to the U.S. population would decrease or increase the risk of radiation carcinogenesis. First, the population survival function acts to decrease radiation risks, especially at older ages. Therefore, an improved survival function acting alone will increase the risk from radiation. However, an improved survival function also suggests lower background cancer rates, making up some fraction of the delay in mortality. In the multiplicative transfer model, radiation risks are reduced by the healthy worker effect, in part due to a reduced natural incidence of cancer. Thus, the portions of risk transfer assigned to multiplicative and additive transfer act in opposition if a healthy worker effect is present. In a model where a geometric average of these two models is used, we expect a minor change if an improved life-table and background cancer rates are assumed. The role of the survival function is also reduced if, as has been suggested in some studies (Preston *et al*., 2003), solid cancers would display a plateau at long times after exposure (>30 y). This discussion points to the need for better understanding of the biological basis for risk transfer models and dependence of risk after long follow-up times.

To estimate the effects of gender- and calendar-year-specific population data on radiation risk projections, **Table 3** shows results for males and females receiving an exposure of 1 Sv where radiation rates are fixed but life-tables and/or cancer rates for females and males, respectively, are varied between the genders. It can be seen that these changes lead to variations of no more than $\pm$20%. The higher cancer risk for females is thus largely due to the additional risks for breast and ovarian cancer, with lifespan differences between genders making a minor contribution. The Social Security Administration (SSA, 2004) has looked at life-expectancy projections over the next 75 years, a time that spans the period of the Mars exploration program. The SSA results, given in **Figure 6,** show about a six-year increase in life-expectancy for males and females over this time period. Since in the year 2000 life-tables females have about a six-year longer life-expectancy than males, the examples shown in **Table 3** for males using the female population rates also serve to illustrate the change expected owing to calendar-year evolution of population rates over the course of the next 75 years. The differences between males and females also suggest the level of change that could occur if healthy worker population rates were modeled. The comparison indicates changes on the order of 10% over the next few decades, but larger changes would occur using a purely multiplicative transfer model.
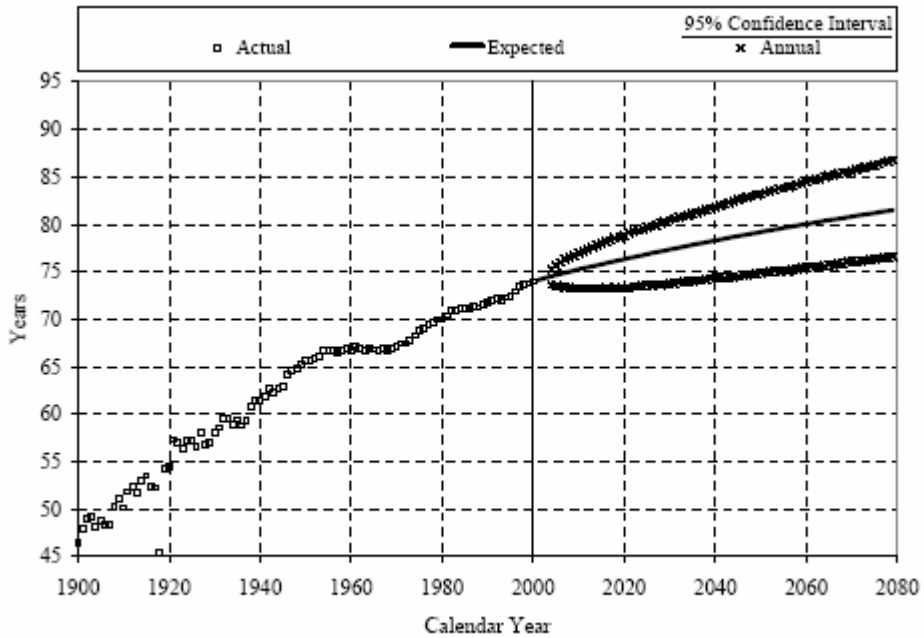
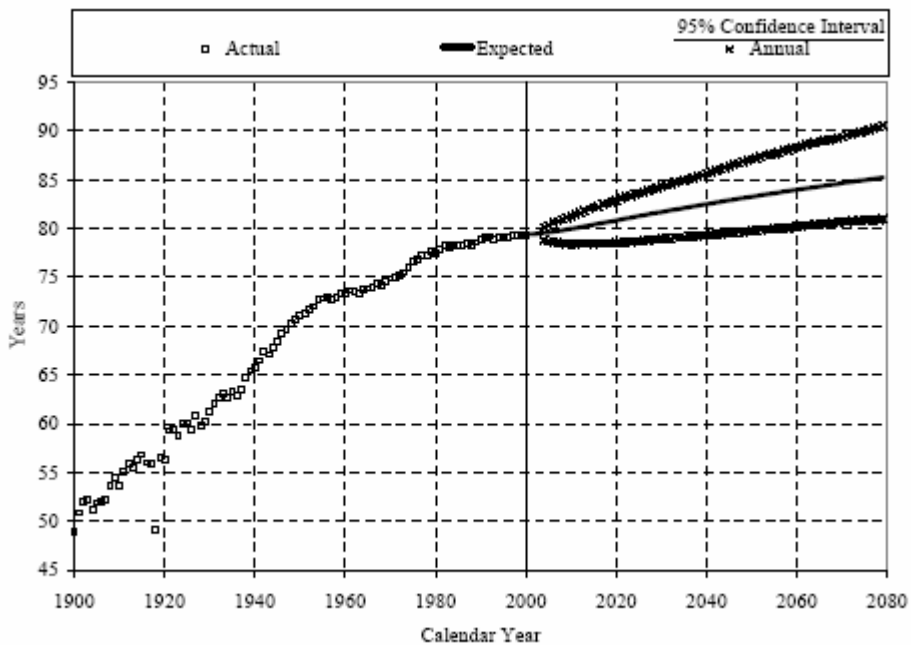**Figure 6a**. Actual or projected male median lifespan at birth vs. calendar year (from SSA, 2004).

Figure 6b. Actual or projected female median lifespan at birth vs. calendar year (from SSA, 2004).

Table 3a. Sensitivity study of REID(%) for *males* at 1-Sv effective dose estimated using *male* radiation rates and *female* life-table and population cancer rates. Percent changes from altering these background rates are listed in parenthesis

Age, yr	Males	Males with female $M(a), M_c(a)$	Males with female $M(a)$	Males with female $M_c(a)$
30	4.84	5.20 (+7.4)	5.99 (+23.8)	4.23 (−12.6)
40	3.76	4.08 (+8.5)	4.63 (+23.1)	3.33 (−11.4)
50	2.59	2.83 (+9.3)	3.21 (+23.9)	2.29 (−11.6)

Table 3b. Same as Table **3a** for females

Age, yr	Females	Females with male $M(a), M_c(a)$	Females with male $M(a)$	Females with male $M_c(a)$
30	6.45	6.24 (−3.3)	5.20 (−19.4)	7.79 (+20.8)
40	4.83	4.63 (−4.1)	3.91 (−19.1)	5.77 (+19.5)
50	3.27	3.13 (−4.3)	2.62 (−19.9)	3.92 (+19.9)

4. Probability Distribution Functions for Space Exploration Missions

The cancer risk projection for space missions is found by folding predictions of the tissue-weighted LET spectra behind spacecraft shielding, dF/dL, with the radiation cancer mortality rate to form a rate for a trial J:

$$m_J(E,a_E,a) \;=\; m_{lJ}(E,a_E,a)\int dL \frac{dF}{dL}LQ_{trial-J}(L)x_{L-J}.$$
(10)

(Not shown are quantiles associated with low-LET mortality rate.) Alternatively, particle-specific energy spectra, $F_j(E)$, for each ion, j, can be used:

$$m_J(E,a_E,a) \;=\; m_{lJ}(E,a_E,a)\sum_j \int dE F_j(E)L(E)Q_{trial-J}(L(E))x_{L-J}$$
(11)

The result of Eq. (10) or (11) is then inserted into the expression for the REID of Eq. (4). In implementing a numerical procedure, we group the PDFs related to the risk coefficient of the normal form, consisting of the dosimetry, bias, and statistical uncertainties, into a combined PDF, $P_{cmb}(x)$. After accumulating sufficient trials ($\sim 10^5$), the results for the REID estimates are binned and the median values and confidence intervals are found.

We use the χ^2 test for determining whether PDFs for two distinct shielding configurations or materials significantly differ. We denote the calculated PDFs for a REID of R_i for two config-urations or materials as $p_1(R_i)$ and $p_2(R_i)$, respectively. Each $p(R_i)$ follows a Poisson distribution with variance, $\sqrt{p(R_i)}$. The chi-squared, χ^2 test for characterizing the dispersion between the two distributions is then

$$\chi^2 \;=\; \sum_n \frac{[p_1(R_n) - p_2(R_n)]^2}{\sqrt{p_1^2(R_n) + p_2^2(R_n)}}.$$
(12)

Once χ^2 is determined, the probability $P(n,\chi^2)$ that the two distributions are the same is calculated. If χ^2 is sufficiently large such that $P(n,\chi^2)$ is less than about 20%, this is an indication that we can conclude that the two distributions lead to distinct cancer risks from GCR and/or SPEs with the material with the lowest mean and upper 95% CL values preferred for radiation protection. However, the opposite result indicates that either the materials are approximately the same, or that the uncertainties in risk models prevent us from concluding that either configuration or material is superior for radiation protection properties. We evaluate χ^2 for the LET-dependent parts of the uncertainties (quality factors and physics) separately, since only these contributions explicitly depend on the modification of radiation fields by shielding.

5. Results

In the results described next, we use values of *ERR* and *EAR* for solid cancers from the Japanese Longitudinal Lifespan Study Report No. 13 (Preston *et al.*, 2003). Note that these values for females were found to about 15% lower than the prior Report No. 12 (Pierce *et al.*, 1996) used by NCRP Report No. 132 (NCRP, 2000) and values for males were nearly the same in Reports 12 and 13. Values for *ERR* and *EAR* for leukemia were not updated in the latest report; we use the values from Pierce *et al.* (1996). We also use life-tables (CDC, 2002 and background cancer mortality rates (SEER, 2000) for the average U.S. population for the year 2000. For models, we use the GCR free space environment of Badhwar *et al.* (1994b), the high charge and energy transport (HZETRN) code (Wilson *et al.*, 1991, 1995), and the QMSFRG model of nuclear fragmentation cross sections (Cucinotta *et al.*, 2003). The CAMERA model (Billings *et al.*, 1973) is used for organ shielding with tissue-weighting coefficients (NCRP, 2000). **Figure 7** shows calculations of the point dose equivalent and the effective dose (tissue averaged organ dose equivalent) for various shielding materials calculated by the HZETRN/BRYNTRN codes for the solar minimum GCR environment and the August 1972 SPE. Calculations predict that the effects of SPE are readily mitigated by shielding (the effects of GCR are not), and that tissue shielding reduces the differences expected when comparing materials. For hydrogen shielding, the GCR effective dose is larger than the point dose because target fragments in tissue contribute about 50% of the effective dose, even though very little secondary radiation is produced directly in the hydrogen shield. Clearly, calculations or measurements of point dose equivalents misrepresent the effectiveness of shielding because of the role of secondary radiation produced in tissue.
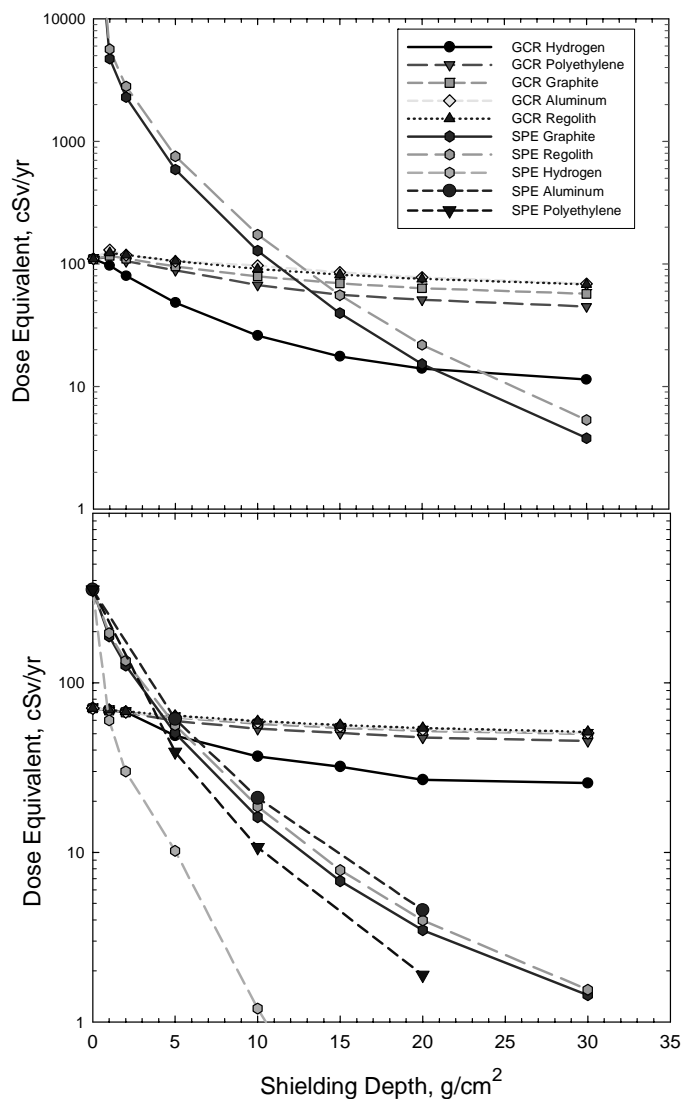
Figure 7. Point dose equivalent (upper panel) and effective dose (bottom panel) behind various shields for solar minimum GCR and August 1972 SPE (the units for the SPE doses are for total event and not necessarily per year).

Spacecraft typically have aluminum as a major constituent, and transport calculations often scale material thicknesses under an aluminum-equivalent areal-density $t=\rho x$, approximation where ρ is mass density, x, is physical thickness, and materials are scaled to aluminum by the ratio of the range of 60 MeV protons or a similar approximation. **Figure 8** shows thickness distributions in aluminum-equivalent depths for the Apollo Command module and several more recent spacecraft used in LEO. Minimal areal-densities of spacecraft such as Skylab, the Space Shuttle, or the International Space Station (ISS) are 2 to 5 g/cm^2; however, averages are in the range from 10–25 g/cm^2 of aluminum-equivalent material. The launch requirements for deep space may require reduced shielding mass compare to these vehicles. Many dose calculations in the scientific literature underestimate the inherent shielding of spacecraft and tissues. For our calculations, we use 5, 10, and 20 g/cm^2 as representative of minimal or average shields. Complex shielding con-

figurations are a superposition of these results (Cucinotta *et al*., 2000), but transition effects between materials should be considered.

Figure 9 shows calculations for the point estimate and 95% CI for risk vs. LET for males exposed at age 40 y. The top panel shows risks at an absorbed dose of 0.01 Gy, and the bottom panel shows risk at an absorbed dose of 0.1 Gy. The solid squares are the resulting "fold-uncertainty" defined as the ratio of the 95% confidence level (CL) to the point estimate. At high LET, a five-fold uncertainty occurs at a low absorbed dose; at a higher absorbed dose and near the peak LET effectiveness, however, the uncertainties are reduced to about three-fold due to competing causes of death limiting the upper levels of risk from radiation. **Figure 10** shows the REID dose response for iron ions (1000 MeV/u) and illustrates how curvature arises due to competing risks.

NASA is considering various lunar and Mars missions as part of its exploration vision. An exploration concept is planned with missions to the Moon and Mars swingby and surface missions, respectively. Approximate characteristics of these missions used in our calculations are described in **Table 4**. Since the variation of GCR and SPE over the solar cycle would be difficult to use as a trade variable in long-term planning, we therefore discuss calculations at solar minimum and near solar maximum. We consider cancer risk calculations for Mars missions. For solar maximum calculations, we assume that the large SPE of August 1972 occurred during the interplanetary part of the mission, and use a solar modulation parameter (Badhwar *et al*., 1994a) of 1100 MV that is typical of about two years past solar maximum, when large SPEs often occur. SPE worst-case risks will be considered in Part II of this series of reports. Note that SPE exposures on the lunar surface are reduced by approximately one-half by the Moon itself, and on the Mars surface by more than one-half due to the planet and the Mars atmosphere. We use a 16 g/cm^2 vertical height for the Mars carbon dioxide atmosphere in our calculations.

Table 4. Summary of mission parameters used for NASA exploration mission risk estimates

Exploration mission	Time period	Total days	Deep space days	Lunar or Mars surface days
LEO CEV test	2012–2015	6	6 (LEO)	0
Lunar-short	2014–2020	14	6	8
Lunar-long	2020–2030	90	6	84
Mars swingby	2030–2040	600	600	0
Mars surface	2030–2040	1000	400	600
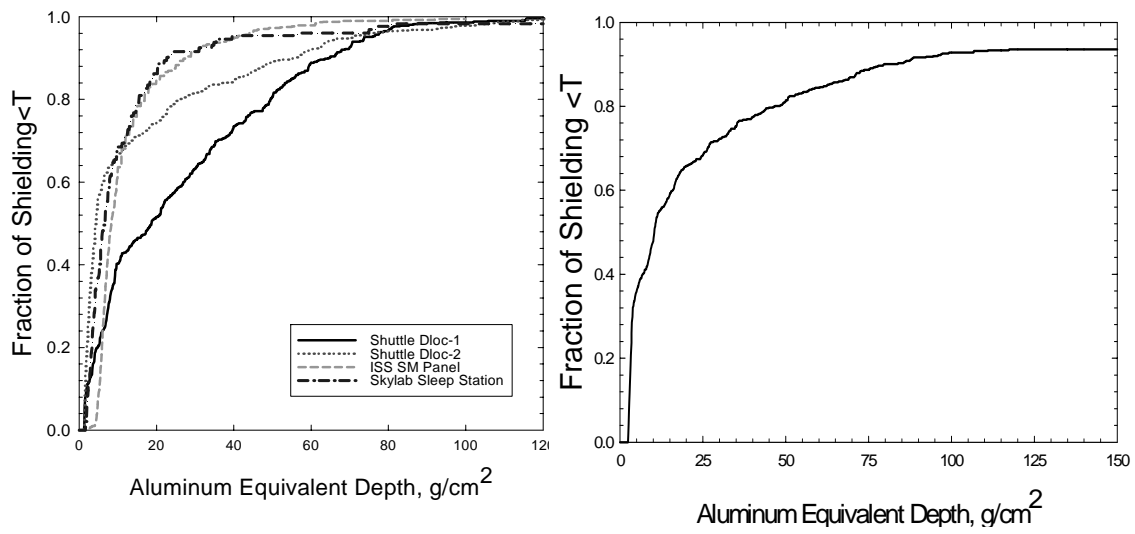
Figure 8. Mass distributions in aluminum-equivalent depths: Left panel in Space Shuttle, ISS Service Module, and Skylab commander sleep compartment; and right panel for Apollo command module.
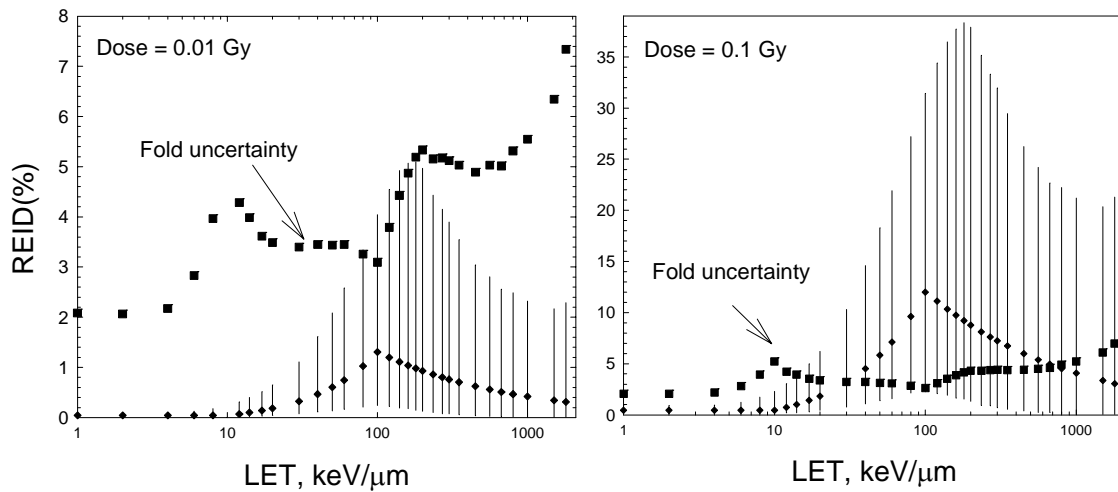
Figure 9. Calculations of REID vs. LET at doses of 0.01 or 0.1 Gy for 40-y males. Diamonds point estimates, bands 95% CI, and squares the fold uncertainties.

19
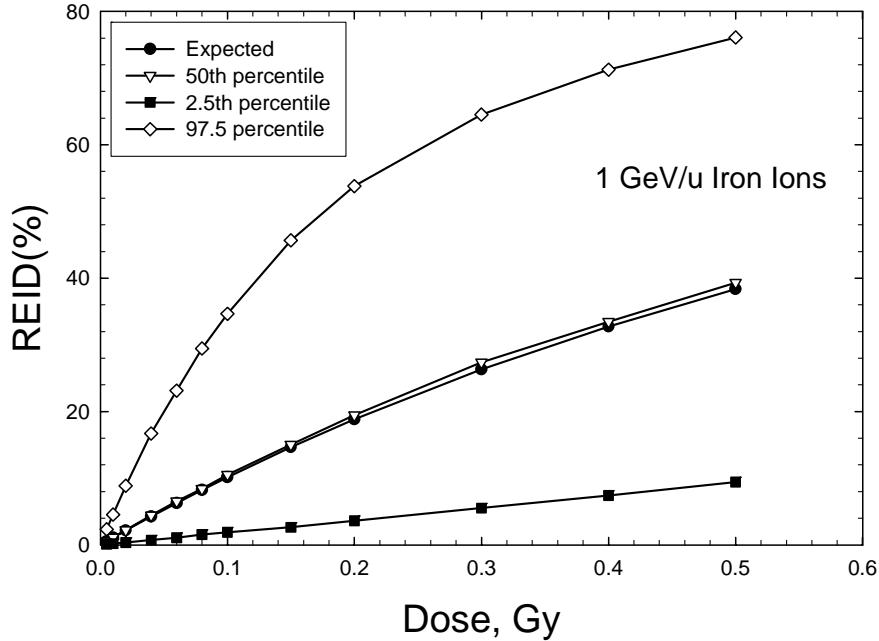
Figure 10. Dose response for point estimate and confidence levels for 1-GeV/u iron ions showing curvature in the response at high risk levels due to competing risks.

      Table 5 shows fatal cancer risk projections at solar minimum for males and females of age 40 y at the time of the mission. Cancer morbidity risks are about 50% higher than mortality risks described here. Calculations are made for minimally shielded spacecraft of 5 g/cm^2 aluminum and a heavily shielded spacecraft of 20 g/cm^2. Similar calculations near solar maximum are shown in **Table 6**; an SPE fluence equivalent to the August 1972 SPE is assumed to have occurred. At solar minimum, it is seen that a four-fold addition of mass reduces the cancer risk by only about 15%. Results differ at solar maximum, where a four-fold increase in shielding mass leads to a more than two-fold reduction in cancer risk; solar protons are less penetrating than GCR and effectively mitigated by shielding. However, for heavy shielding ($\geq$ 20 g/cm^2), GCR dominates over SPEs and further addition of shielding provides marginal reductions. Each SPE is unique in that it has distinct fluence, energy spectra, and dose rates; therefore, the shielding thickness where GCR doses exceed SPE doses varies from event to event.

Table 5a. Calculations of effective doses, REID, and 95% CI for lunar or Mars missions. Calculations are at solar minimum for a 5-g/cm^2 aluminum shield

Exploration mission	D, Gy	E, Sv	REID(%)	95% CI
			Males (40 y)	
Lunar-long	0.03	0.084	0.34	[0.10, 1.2]
Mars swingby	0.37	1.03	4.0	[1.0, 10.5]
Mars surface	0.42	1.07	4.2	[1.3, 13.6]
			Females (40 y)	
Lunar-long	0.03	0.084	0.41	[0.12, 1.5]
Mars swingby	0.37	1.03	4.9	[1.4, 16.2]
Mars surface	0.42	1.07	5.1	[1.6, 16.4]

Table 5b. Calculations of effective doses, REID, and 95% CI for lunar or Mars missions. Calculations are at solar minimum for a 20-g/cm^2 aluminum shield

Exploration mission	D, Gy	E, Sv	REID(%)	95% CI
			Males (40 y)	
Lunar-long	0.03	0.071	0.28	[0.09, 0.95]
Mars swingby	0.36	0.87	3.2	[1.0, 10.4]
Mars surface	0.41	0.96	3.4	[1.1, 10.8]
			Females (40 y)	
Lunar-long	0.03	0.071	0.34	[0.11, 1.2]
Mars swingby	0.36	0.87	3.9	[1.2, 12.7]
Mars surface	0.41	0.96	4.1	[1.3, 13.3]

Table 6a. Calculations of effective doses, REID, and 95% CI for lunar or Mars missions. Calculations are near solar maximum assuming 1972 SPE in deep space segment of mission with a 5-g/cm^2 aluminum shield

Exploration mission	D, Gy	E, Sv	REID(%)	95% CI
			Males (40 y)	
Lunar-long	0.45	0.69	2.7	[0.95, 7.6]
Mars swingby	0.62	1.21	4.4	[1.5, 13.1]
Mars surface	0.66	1.24	4.8	[1.6, 14.2]
			Females (40 y)	
Lunar-long	0.45	0.69	3.3	[1.1, 9.3]
Mars swingby	0.62	1.21	5.7	[1.8, 17.1]
Mars surface	0.66	1.24	5.8	[2.0, 17.3]

Table 6b. Calculations of effective doses, REID, and 95% CI for lunar or Mars missions. Calculations are near solar maximum assuming 1972 SPE in deep space segment of mission with a 20-g/cm^2 aluminum shield

Exploration mission	D, Gy	E, Sv	REID(%)	95% CI
			Males (40 y)	
Lunar-long	0.04	0.09	0.36	[0.12, 1.2]
Mars swingby	0.22	0.54	2.0	[0.60, 6.8]
Mars surface	0.25	0.60	2.4	[0.76, 7.8]
			Females (40 y)	
Lunar-long	0.04	0.09	0.43	[0.13, 1.4]
Mars swingby	0.22	0.54	2.5	[0.76, 8.3]
Mars surface	0.25	0.60	2.9	[0.89, 9.5]

An alternative to a shielding approach that adds mass is to optimize materials used in spacecraft structures or planetary habitats to reduce radiation risk. **Figure 11** shows PDFs for the GCR as solar minimum for aluminum, polyethylene, and liquid hydrogen shielding with areal density of 20 g/cm^2. **Table 7** shows results for the χ^2 statistic comparing polyethylene and hydrogen shielding effectiveness to aluminum. For calculations that ignore the low-LET risk coefficient uncertainties, near solar maximum with a large SPE, significant results ($P<0.01$) are found for liquid hydrogen and for the GCR at solar minimum (with $P<0.15$). We conclude that, because of the modest differences between polyethylene and aluminum as GCR absorbers and the large radiobiological uncertainties in cancer risk projection models, the benefits of polyethylene compared to aluminum shielding for GCR cannot be proven at this time. A key factor in these results

is that, although aluminum is a greater producer of secondary radiation compared to polyethylene, tissue shielding "equalizes" many of these differences.

The formalism can be applied to estimate the number of days a mission is ensured to be below an exposure limit at a given confidence level. Because we use the REID quantity and the newer Life-Span Study of the Atomic-Bomb Survivors, LSS Report 13 (Preston *et al*., 2003) values for ELR and EAR compared to NCRP Report 132 (NCRP, 2000) and consider limits for single missions rather than 10-year careers, we first calculated dose limits that result for the present model corresponding to 3% and 5% fatal cancer risk for missions of length <3 y. These are listed in **Table 8**, which also shows calculations of LLE from radiation-induced cancers. In an earlier report (Cucinotta, *et al*., 2000b), we estimated the maximum number of days in deep space that astronauts could spend with a 95% CL to remain below a 3% fatal cancer risk. **Table 9** updates these calculations and compares them to the earlier report. These results show a significant increase in the number of "safe" days, with 95% CL to remain below acceptable levels or risk that result from our improved methodology. However, the results still fall well short of those needed for a Mars mission.
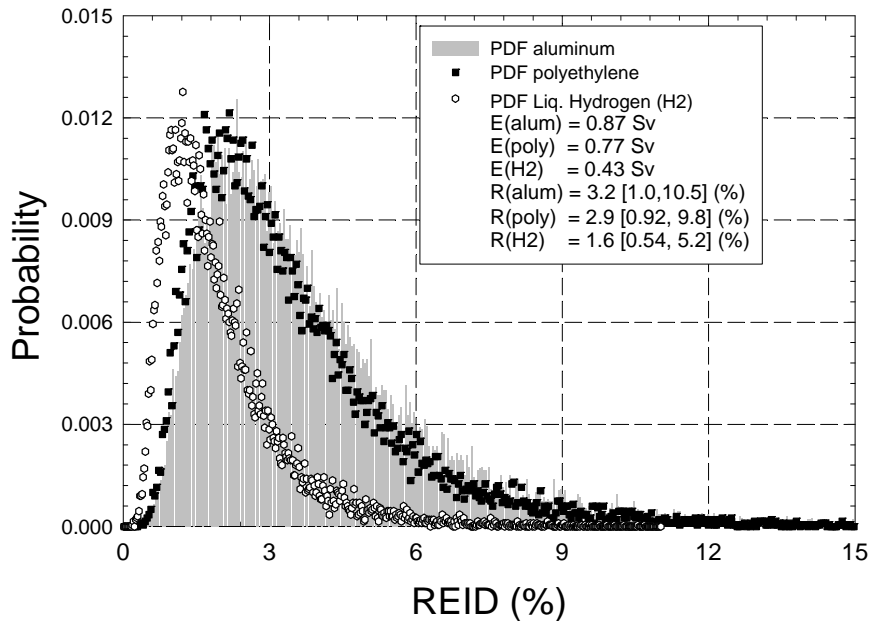

Figure 11. PDFs for 40-y males on Mars swingby mission of 600 days for 20-g/cm^2 shields of aluminum, polyethylene, or liquid hydrogen. Effective doses, point estimates, and 95% CI for REID are shown in box.

23

Table 7a. χ^2 test at solar minimum for 20- g/cm^2 shields for 40-y males on Mars swingby mission. $P(n, \chi^2)$ is the probability materials cannot be determined to be significantly different (n=500). Values in bold for $P(n, \chi^2)$<0.2 indicate a significant improvement over aluminum

Test Material	E, Sv	REID(%)	95% CL	χ^2/n	$P(n,\chi^2)$
			All uncertainties		
Aluminum	0.87	3.2	[1.0, 10.5]	–	–
Polyethylene	0.78	2.9	[0.94, 9.2]	0.05	>0.99
Hydrogen	0.43	1.6	[0.52, 5.1]	0.63	>0.99
			LET-dependent uncertainties		
Aluminum	0.87	3.2	[1.9, 8.7]	–	–
Polyethylene	0.78	2.9	[1.8, 7.5]	0.08	>0.99
Hydrogen	0.43	1.7	[1.0, 4.2]	**1.10**	**<0.15**

Table 7b. Same as **Table 7a** near solar maximum for 5-g/cm^2 shields

Test Material	E, Sv	REID(%)	95% CL	χ^2/n	$P(n,\chi^2)$
			All uncertainties		
Aluminum	1.21	4.4	[1.5, 13.1]	–	–
Polyethylene	0.94	3.5	[1.2, 10.8]	0.14	>0.99
Hydrogen	0.52	2.1	[0.60, 6.4]	0.81	>0.99
			LET-dependent uncertainties		
Aluminum	1.21	4.4	[3.0. 11.0]	–	–
Polyethylene	0.94	3.5	[2.3, 8.8]	0.32	>0.99
Hydrogen	0.52	2.1	[1.2, 5.2]	**1.38**	**<0.001**

Table 7c. Same as **Table 7a** near solar maximum for 20-g/cm^2 shields

Test Material	E, Sv	REID(%)	95% CL	χ^2/n	$P(n,\chi^2)$
			All uncertainties		
Aluminum	0.54	2.0	[0.60, 6.8]	–	–
Polyethylene	0.45	1.7	[0.52, 5.6]	0.08	>0.99
Hydrogen	0.24	0.9	[0.27, 2.9]	0.77	>0.99
			LET-dependent uncertainties		
Aluminum	0.54	2.0	[1.2, 5.6]	–	–
Polyethylene	0.45	1.7	[1.0, 4.6]	0.15	>0.99
Hydrogen	0.24	0.9	[0.52, 2.4]	**1.26**	**<0.005**

Table 8a. Example career effective dose limits in units of Sievert for one-year missions and corresponding average life-loss for an exposure-induced death

	E, Sv for 3% REID (average life loss per death, y)	
Age, y	Males	Females
25	0.5 (15.7)	0.4 (15.9)
30	0.6 (15.4)	0.5 (15.7)
35	0.7 (15.0)	0.55 (15.3)
40	0.8 (14.2)	0.6 (14.7)
45	0.95 (13.5)	0.75 (14.0)
50	1.15 (12.5)	0.9 (13.2)
55	1.5 (11.5)	1.1 (12.2)

Table 8b. Example career effective dose limits in units of Sievert for one-year missions and corresponding average life-loss for an exposure-induced death

Age, y	E, Sv for 5% REID (average life loss per death, y)	
	Males	Females
25	0.9 (15.7)	0.6 (15.9)
30	1.0 (15.4)	0.8 (15.7)
35	1.2 (15.0)	0.9 (15.3)
40	1.3 (14.2)	1.0 (14.7)
45	1.6 (13.5)	1.25 (14.0)
50	1.9 (12.5)	1.5 (13.2)
55	2.45 (11.5)	1.9 (12.2)

Table 9a. Projections for males of age-dependent maximum days in deep space with 95% CL of remaining below a risk limit, R_L(%). Calculations are for GCR at solar minimum with 10-g/cm^2 aluminum shielding comparing previous results (Cucinotta *et al.*, 2001b) to present results

Age, y	Previous R_L=3%	Present R_L= 3%	Present R_L= 5%
30	91	142	236
35	104	166	277
40	122	186	310
45	148	224	373
50	191	273	455
55	268	340	568

Table 9b. Projections for females of age-dependent maximum days in deep space with 95% CL of remaining below a risk limit, R_L(%). Calculations are for GCR at solar minimum with 10-g/cm^2 aluminum shielding comparing previous results (Cucinotta *et al.*, 2001b) to present results

Age, y	Previous R_L=3%	Present R_L= 3%	Present R_L= 5%
30	54	112	187
35	62	132	220
40	73	150	250
45	89	182	304
50	115	224	374
55	159	282	470

6. Discussion and Recommendations

The building of PDFs that propagate errors from individual factors that contribute to uncertainties in projection models is a powerful tool for managing radiation risks, including evaluating benefits of research and mitigation approaches and implementing the radiation protection principle of as low as reasonable achievable (ALARA). The uncertainties estimated here are reduced compared to our previous estimates (Cucinotta *et al.*, 2001b, 2002, 2004) for the following reasons:

1. Use of the REID rather than radiation cancer rates (decreases upper uncertainty level because of role of competing risks).
2. Use of trial *Q(L)* functions rather than uncorrelated uncertainties as a function of LET (overall decrease in uncertainties).
3. Neglect of NCRP "unknown" uncertainties (decrease in uncertainties).
4. Redefining LET spectra uncertainties (modest increase in uncertainties).

However, these estimates should be viewed as preliminary because of the need to assess additional uncertainties that have not been included in the analysis, including protraction effects, scaling of ERRs or EARs estimated from low-LET data to high LETs, and the potential impact of a healthy worker effect. These factors will need to be considered in future work. Research at the NSRL will have a major impact on reducing uncertainties by establishing a basic understanding for extrapolating experimental data to humans, and by providing important data for reducing the major uncertainties described above (i.e., dose-rate effects and quality factors). Low-LET epidemiology data and physics models uncertainties have a smaller role in the present evaluation. As noted in our earlier report (Cucinotta *et al.*, 2001b), other uncertainties exist in the representation of radiation shielding composition and predicting future solar cycle effects or the characteristics of SPEs; however, these are more practical in nature and will be considered elsewhere.

The methodologies used for risk assessment ultimately play a large role in the estimates of uncertainties and shielding effectiveness. The use of the linear-additivity model is a key assumption in the current methodology. This model has a strong theoretical basis and is consistent with mouse carcinogenesis studies with low-dose neutron irradiations (Storer and Fry, 1995). For neutron exposures, a mixed low- and high-LET field is present due to the gamma-ray component produced by neutrons and this would not be representative of the spectral and temporal patterns of GCR. Possible deviations from the linear-additivity model for the GCR spectrum along with correlations in estimates of DDREF, protraction effects, and quality factors need to be considered in future work. Experiments that simulate the constant high-energy proton background and variable dose-rate SPEs with interspersed heavy nuclei irradiation such as iron would be a first step in testing these effects. The NCRP model (NCRP, 2000) applies a DDREF of only two for total doses less than 200 mGy or dose-rates less than 0.1 mGy/min. The former condition is not met for the Mars missions or for a large SPE, and should be investigated in future work. Further investigation of alternative methodologies that could possibly reduce uncertainty estimates should also be considered. The use of Bayesian statistics combined with track structure models to explore the replacement of $Q(L)$ functions with Q functions dependent on charge and LET or kinetic energy, and the resulting effects on uncertainties will also be described in a future report. Alternative methodologies, including ones that study cancer incidence at specific tissue sites, should allow additional biological factors to enter risk models—perhaps lowering uncertainty estimates. However, the need for new biological data and understanding is the most important approach to reducing uncertainties.

For exploration missions outside LEO, higher risks from radiation may be unavoidable because of the longer durations where high GCR exposures will occur and the potential risks from SPEs. In this report we have discussed radiation limits using the alternative quantity REID instead of the ELR of fatal cancer used in the past. The REID is recommended because it is more directly comparable to other mission risks, especially when supplemented with information on the average life-loss per death, LLER. The LLER estimates provided in **Table 8** are likely lower bounds because high-LET radiation effects are known to occur with reduced latency compared to gamma-rays from which these estimates are based. Research to make accurate estimates of LLER values as a function of exposure and tumor type will be important for mission risk assessments.

Career radiation limits and shielding requirements could also be impacted by new knowledge of fatal non-cancer risks from radiation exposure such as heart disease (Preston *et al.*, 2003; Howe *et al.*, 2004; Yang and Ainsworth, 1982) or damage to the CNS. Based on the Japanese survivor data (Preston *et al.*, 2003), non-cancer risks are estimated to be small for the shorter lunar missions, but could lead to a significant risk for a Mars mission. The risk of heart disease for ions is largely unknown because only one report (considered a pilot study by its authors) has been made on the effects of HZE ions on heart disease (Yang and Ainsworth, 1982),

and human data for low-LET radiation at low dose-rates is inconclusive on the level of risk to be expected (Howe *et al*., 2004; Cardis *et al*., 1995). CNS risks have the potential to impact both short-term and career radiation limits and mitigation approaches (NRC, 1996), but it will be several years before radiobiological research will provide sufficient knowledge on CNS risks to be used operationally by NASA.

As new experimental data and models of cancer risks are obtained from the NSRL, we expect to see a significant reduction in estimates of uncertainties compared to the estimates cited in this report. There are, however, limitations on the extent of uncertainty reduction that can be achieved by using population-based estimates. In future, the need for performing individual-based risk assessment will grow if uncertainties less than about two-fold are to be achieved. A major conclusion of this report is that funding of ground-based space radiobiology research to reduce the uncertainties in risk projections remains the most cost-effective approach for achieving goals in radiation safety, including ensuring that risk mitigation approaches are validated.

We have shown that, with regard to the GCR, the optimization of material selection and mass cannot be put on a sound scientific basis because the reductions estimated from point estimates alone are only on the order of 10–30% for most shielding materials, and, when combined with uncertainties in projection models, non-significant results for risk reduction are found. It still may be reasonable to assume that risk is reduced when comparing hydrocarbon shields to aluminum or other metals, but application of ALARA is problematic since a cost-benefit analysis cannot be properly performed under these conditions. In contrast, for acute risks, which are largely an absorbed dose and dose-rate effect, SPEs are the major concern and the role of minimizing mass requirements through hydrocarbon shielding materials is easier to prove. We therefore recommend the following approach for radiation shielding designs until uncertainties are reduced to a degree that significance testing of shielding effectiveness can be based on PDFs:

1. Exploration vehicles should be designed to reduce acute radiation risks from SPEs to well below a 30-day limit of 0.25 Gy-Eq using a worst-case SPE environment that will be discussed in Part II of this report.
2. Secondary to SPE shielding should be the optimization of GCR shielding. A reduction of the following three quantities by more than 25% compared to aluminum should be considered to demonstrate sufficient value in alternative shielding materials:
   a. Effective dose (organ averaged).
   b. HZE fluence, $F(E)$ for ions with $Z>10$.
   c. $F(L)$ for $L>30$ keV/μm.
   d. Neutron fluence, $F(E)$ between 0.1 to 20 MeV.

The requirements in (a) through (d) above are partially redundant but are needed to ensure that the radiation components with the highest biological uncertainties are significantly reduced when evaluating GCR shielding concepts. Reductions of less than 25% could be considered if the costs for their implementation are low.

The ALARA principle is an important aspect of radiation safety. Our estimate of 95% CLs to stay below limits can be used as criteria for a minimal ALARA requirement for the design of lunar missions, including transfer vehicle or surface habitat designs. For example, about a four-fold margin can be used for GCR exposures and about a 2.5-fold margin can be used for SPEs. Detailed cost-benefit analysis should be used for measures that would provide even lower risks. Future work should consider a worst-case SPE environment, including the possibility of multiple SPEs as a function of mission duration. Based on the results of **Table 9** and the above margins,

27

we conclude that "blind selection" of astronauts for lunar missions can be made for missions with a duration of fewer than 180 days for male or female astronauts above the age of 35 y if sufficient protection against SPEs is provided. Because of the higher GCR risks for Mars exploration and the likely impacts of non-cancer risks, no conclusions on ALARA goals for these missions or the possibility of "blind selection" can be made at this time. The inherent uncertainties in population-based risk models and the higher risks on long-duration missions point to the likelihood that individual-based risk assessments will be needed for Mars exploration missions.

7. References

Ainsworth, E.J., Early and Late Mammalian Responses to Heavy Charged Particles. *Adv. in Space Res.* **6**, 153–162, 1986.

Alpen, E.L., Powers-Risius, P, Curtis, S.B., DeGuzman, R., Tumorigenic Potential of High-Z, High-LET Charged Particle Radiations. *Radiat. Res.* **88**, 132–143, 1993.

Alpen, E.L., Powers-Risius, P., Curtis, S.B., DeGuzman, R., Fry, R.J.M., Fluence-Based Relative Biological Effectiveness for Charged Particle Carcinogenesis in Mouse Harderian Gland. *Adv. Space. Res.* **14(10),** 573–581, 1994.

Badhwar, G.D., O'Neill, P.M., Long-term Modulation of Galactic Cosmic Radiation and Its Model for Space Exploration. *Adv. Space. Res*. **14(10),** 749–757, 1994a.

Badhwar, G.D., Cucinotta, F.A., O'Neill, P.M., An Analysis of Interplanetary Space Radiation Exposure for Various Solar Cycles. *Radiat. Res.* **138**, 201–208, 1994b.

Badhwar, G.D, Spaceflight Validation of Material Shielding Properties. In: NASA Workshop on Shielding Strategies for Human Space Exploration. Eds. Wilson, J.W., Miller, J., Konradi, A., and Cucinotta, F.A. NASA-CP-1997-3360.

Badhwar, G.D., Cucinotta, F.A., A Comparison of Depth Dependence of Dose and Linear Energy Transfer Spectra in Aluminum and Polyethylene. *Radiat. Res.* **153**, 1–8, 2000.

Belli M., Cera F., Cherubini, R., Haque, A.M.I., Ianzini, F., Moschini, G., Sapora, O., Simone, G. Tabocchini, M.A., Tiverton, P., Inactivation and Mutation Induction In V79 Cells by Low Energy Protons: Re-evaluation of the results at the LNL facility. *Int. J. Radiat. Biol*. **63**, 331–337, 1993.

Billings, M.P., Yucker, W.R., Heckman, B.R., Body Self-Shielding Data Analysis, McDonald Douglas Astronautics Company West, MDC-G4131, 1973.

Bunger, B.M., Cook, J.R., Barrick, M.K., Life Table Methodology for Evaluating Radiation Risk: An Application Based On Occupational Exposures. *Health Phys.* **40**, 439–455, 1981.

Burns F., Yin Y., Garte, S.J., Hosselet, S., Estimation of Risk Based on Multiple Events in Radiation Carcinogenesis of Rat Skin. *Adv. Space Res.* **14**, 507–519, 1994.

Cardis, E., *et al.*, Effects of Low Doses and Dose-Rates of External Ionizing Radiation: Cancer Mortality Among Nuclear Industry Workers In Three Countries. *Radiat. Res.* **142**, 117–132, 1995.

Center for Disease Control (CDC) National Vital Statistics Report, Vol. 51, No. 3, US Life Tables, 2000, 2002.

Committee on the Biological Effect of Ionizing Radiation (BEIR) BEIR V, 1994.

Cox, R., Masson, W.K., Mutation and Inactivation of Cultured Mammalian Cells Exposed to Beams of Accelerated Heavy Ions. *Int. J. Radiat. Biol.* **36**, 149–160, 1979.

Cucinotta, F.A., Wilson J.W., Shavers M.R., Katz, R., Effects of Track Structure and Cell Inactivation on the Calculation of Heavy Ion Mutation Rates in Mammalian Cells. *Int. J. Radiat. Biol.* **69**, 593–600, 1996.

Cucinotta, F.A., Wilson, J.W., Shinn, J.L., Tripathi, R.K., Assessment and Requirements of Nuclear Reaction Data Bases for GCR Transport in the Atmosphere and Structures. *Adv. in Space. Res.* **21**, 1753–1762, 1998a.

Cucinotta, F.A., Nikjoo, H., Goodhead, D.T., The Effects of Delta Rays on The Number of Particle-Track Traversals per Cell in Laboratory and Space Exposures. *Radiat. Res.* **150**, 115–119, 1998b.

Cucinotta, F.A., Wilson, J.W., Williams, J.R., Dicello, J.F., Analysis Of Mir-18 Results for Physical And Biological Dosimetry: Radiation Shielding Effectiveness in LEO. *Radiat. Meas.* **31**, 2000.

Cucinotta, F.A., Manuel, F., Jones, J., Izsard G., Murray, J., Djojonegoro B., Wear M., Space Radiation and Cataracts in Astronauts. *Radiat. Res.* **156**, 460–466, 2001a.

Cucinotta, F.A., Schimmerling, W., Wilson, J.W., Peterson, L.E., Saganti, P., Badhwar, G.D., Dicello, J.F., Space Radiation Cancer Risks and Uncertainties for Mars Missions. *Radiat. Res.* **156**, 682–688, 2001b.

Cucinotta, F.A., Badhwar, G.D., Saganti, P., Schimmerling, W., Wilson, J.W., Peterson, L., Dicello, J., Space Radiation Cancer Risk Projections for Exploration Missions, Uncertainty Reduction and Mitigation. NASA TP-2002-210777.

Cucinotta, F.A., Saganti, P.B., Hu, X., Kim, M-H. Y., Cleghorn, T.F., Wilson, J.W., Tripathi, R.K., Zeitlin, C.J., Physics of the Isotopic Dependence of Galactic Cosmic Ray Fluence Behind Shielding. NASA TP-2003-210792.

Cucinotta, F.A., Schimmerling, W., Wilson, J.W., Peterson, L.E., Saganti, P.B., Uncertainties in Estimates of the Risks of Late Effects from Space Radiation. *Adv. Space Res.* **32**, 1383–1389, 2004.

Dicello, J.F., *et al.*, *In vivo* Mammary Tumorigenesis in the Sprague-Dawley Rat and Microdosimetric Correlates. *Phys. Med. Biol.* **49**, 3817–3830, 2004.

Fry, R.J.M., Powers-Risius, P., Alpen, E.L., Ainsworth, E.J., High LET Radiation Carcinogenesis. *Radiat. Res.* **104**, S188–195, 1985.

George, K., Willingham, V., Wu, H., Gridley, D., Nelson, G., Cucinotta, F.A., Chromosome Aberrations in Human Lymphocytes Induced By 250 MeV Protons: Effects of Dose, Dose Rate and Shielding. *Adv. Space Res.* **30**, 891-899, 2002.

George, K., Durante, M., Willingham, V., Wu, H., Yang, T., Cucinotta, F.A., Biological Effectiveness of Accelerated Particles for the Induction of Chromosome Damage Measured in Metaphase and Interphase Human Lymphocytes. *Radiat. Res.* **160**, 425–435, 2003.

Howe, G.R., Zablotska, L.B., Fix, J.J., Egel, J, Buchanan, J., Analysis of the Mortality Experience amongst U.S. Nuclear Power Industry Workers after Chronic Low-Dose Exposure to Ionizing Radiation**.** *Radiat. Res.* **162**, 517–526, 2004.

International Commission on Radiation Units, The Quality Factor in Radiation Protection, ICRU Report 40, ICRU Publications, Bethesda MD, 1986.

International Commission on Radiation Protection, ICRP Publication 92, Relative Biological Effectiveness (RBE), Quality Factor (Q), and Radiation Weighting Factor (w_R), Pergamon, 2003.

Katz, R., Ackerson, B., Homayoonfar, M., Scharma, S.C., Inactivation of Cells by Heavy Ion Bombardment. *Radiat. Res.* **47***,* 402–425, 1971.

Kawata, T., Durante, M., Furusawa, Y., George, K., Takai, N., Wu, H., Cucinotta, F.A., Dose Response of Initial G2-Chromosomal Damage Induced in Normal Human Fibroblasts by High-LET Particles. *Int. J. Radiat. Biol.* **77**, 165–174, 2001.

Kiefer, J., Stoll, U., Schneider, E., Mutation Induction by Heavy Ions. *Adv. Space Res*. **14(10)**, 257–265, 1994.

Kim, M.Y., Barber, R.E., Shavers, M.R., Nikjoo, H., Cucinotta, F.A., TEPCs Overestimate the Average Quality Factor for Trapped Protons and Underestimate the Average Quality Factor for GCR. Presented at the 14th Annual Space Radiation Health Investigators Workshop, 2003.

Kronenberg, A., Mutation Induction in Human Lymphoid Cells by Energetic Heavy Ions. *Adv. Space Res.* **14(10)**, 339–346, 1994.

Martin, S.G., Miller, R.C., Geard, C.R., Hall, E.J., The Biological Effectiveness Of Radon-Progeny Alpha Particles. IV. Morphological Transformation of Syrian Hamster Embryo Cells at Low Dose. *Radiat. Res.* **142**, 70–77, 1995.

Miller, R.C., Marino, S.A., Brenner, D.J., Martin, S.G., Richards, M., Randers-Pehrson, G., Hall, E.J., The Biological Effectiveness of Radon-Progeny Alpha Particles III. Quality Factors. *Radiat. Res.* **142**, 61–69, 1995.

National Academy of Sciences, NAS. National Academy of Sciences Space Science Board, Report of the Task Group on the Biological Effects of Space Radiation. Radiation Hazards to Crews on Interplanetary Mission National Academy of Sciences, Washington, D.C., 1996.

National Council of Radiation Protection and Measurements, NCRP. Relative Biological Effectiveness of Radiations of Different Quality, NCRP Report 104, Bethesda MD, 1990.

National Council on Radiation Protection and Measurements, NCRP. Uncertainties in Fatal Cancer Risk Estimates Used in Radiation Protection, NCRP Report 126, Bethesda MD, 1997.

National Council on Radiation Protection and Measurements, NCRP. Recommendations of Dose Limits for Low Earth Orbit. NCRP Report 132, Bethesda MD, 2000.

Nelson, G.A., Schubert, W.W., Marshall, T.M., Benton, E.R., Benton, E.V., Radiation effects in *Caenorhabditis Elegan*s, Mutagenesis by High and Low LET Ionizing Radiation. *Mut. Res.* **212**, 181–192, 1989.

Nikjoo, H., O'Neill, P., Terrissol, M., Goodhead, D.T., Quantitative Modeling of DNA Damage Using Monte Carlo Track Structure Method. *Radiat. Envir. Biophys.* **38**, 31–38, 1999.

Nikjoo, H., Khvostunov, I.K., Cucinotta, F.A., The Response of (TEPC) Proportional Counters to Heavy Ions. *Radiat. Res.* **157**, 435–445, 2002.

O'Neill, P., Badhwar-O'Neill Galactic Cosmic Ray Model Update Based on Advanced Composition Explorer (ACE) Spectra from 1997 to Present. *Adv. Space Res* (in press), 2005.

Parker, E.N., The Passage of Energetic Charged Particles Through Interplanetary Space. *Planet. Space Sci.* **13**, 9–49, 1965.

Pierce, D.A., Shimizu, Y., Preston, D.L., Vaeth, M., Mabuchi, K., Studies of the Mortality of the Atomic-Bomb Survivors, Report 12, Part I. Cancer: 1950–1990. *Radiat. Res.* **146**, 1–27, 1996.

Preston, D.L., Shimizu, Y., Pierce, D.A., Suyumac, A., Mabuchi, K., Studies of Mortality of Atomic Bomb Survivors. Report 13: Solid Cancer and Noncancer Disease Mortality: 1950–1997. *Radiat. Res.* **160**, 381–407, 2003.

SEER, Surveillance, Epidemiology, and End Results: Cancer Statistics Review, 1973–2000. Cancer Surveillance Research Program, National Cancer Institute, Bethesda MD, 2000.

Shinn, J.L., Cucinotta, F.A., Simonsen, L.C., Wilson, J.W., Badavi, F.F., Badhwar, G.D., Miller, J., Zeitlin, C. R.K., Clowdsley, M.S., Heinbockel, J.H., Xapsos, M.A., Validation of a Comprehensive Space Radiation Transport Code. *IEEE Nuclear Sci.* **45**, 2711–2719, 1998.

Social Security Administration (SSA), A Stochastic Model of the Long-Range Financial Status of the OASDI Program Actuarial Study No. 117. Social Security Administration, Office of the Chief Actuary September 2004 SSA Pub. No. 11-11555.

Storer, J.B., Fry, R.J.M., Limiting Values of RBE of Fission Neutrons at Low Doses for Life-Shortening in Mice. *Radiat. Environ. Biophys*. **34**, 21–27, 1995.

Tsuboi, K., Yang, T.C., Chen, D.J., Charged-particle mutagenesis-I. cytoxic and mutagenic effects of high-LET charged ion particles on human skin fibroblasts. *Radiat. Res.* **129**, 171–176, 1992.

Ullrich, R.L., Tumor Induction in BAL/c Mice after Fractionated Neutron or Gamma Irradiation. *Radiat. Res*. **93**, 506–512, 1984.

Ullrich, R.L., Ponnaiya B., Radiation-Induced Instability and Its Relation to Radiation Carcinogenesis. *Inter. J. Radiat. Biol.* **74**, 747–754, 1998.

Vaeth, M., Pierce, D.A., Calculating Excess Lifetime Risk in Relative Risk Models. *Environ. Health Per.* **87**, 83–94, 1990.

Wilson J.W., Townsend, L.W., Schimmerling, W., Khandelwal, G.S., Khan, F., Nealy, J.E., Cucinotta, F.A., Simonsen, L.C., Norbury, J.W., Transport Methods and Interactions for Space Radiations. RP1257, NASA, Washington D.C., 1991.

Wilson, J. W., Kim, M., Schimmerling, W., Badavi, F. F., Thibeault, S. A., Cucinotta, F. A., Shinn, J. L., Kiefer, R., Issues in Space Radiation Protection. *Health Phys.* **68**, 50–58, 1995.

Yang, V.V., Ainsworth, E.J., Late Effects of Heavy Charged Particles on the Fine Structure of the Mouse Coronary Artery. *Radiat. Res.* **91**, 135–144, 1982.

Yang, T.C., Craise, L.M., Mei, M., Tobias, C.A., Neoplastic Transformation by High LET Radiation: Molecular Mechanisms. *Adv. Space. Res.* **9**, 131–140, 1989.

REPORT DOCUMENTATION PAGE	Form Approved OMB No. 0704-0188

1. AGENCY USE ONLY *(Leave Blank)*	2. REPORT DATE July 2005	3. REPORT TYPE AND DATES COVERED NASA Technical Paper	

4. TITLE AND SUBTITLE
Managing Lunar and Mars Mission Radiation Risks
Part I: Cancer Risks, Uncertainties, and Shielding Effectiveness

5. FUNDING NUMBERS

6. AUTHOR(S)
Francis A. Cucinotta*, Myung-Hee Y. Kim**, Lei Ren***

7. PERFORMING ORGANIZATION NAME(S) AND ADDRESS(ES)

*NASA Lyndon B. Johnson Space Center; **Wyle Laboratories; ***U.S.R.A. Division of Space Life Science Division

8. PERFORMING ORGANIZATION REPORT NUMBERS
S-960

9. SPONSORING/MONITORING AGENCY NAME(S) AND ADDRESS(ES)

National Aeronautics and Space Administration
Washington, DC 20546-0001

10. SPONSORING/MONITORING AGENCY REPORT NUMBER
TP-2005-213164

11. SUPPLEMENTARY NOTES

12a. DISTRIBUTION/AVAILABILITY STATEMENT

Unclassified/Unlimited
Available from the NASA Center for AeroSpace Information (CASI)
7121 Standard
Hanover, MD 21076-1320   Category: 52

12b. DISTRIBUTION CODE

13. ABSTRACT *(Maximum 200 words)*

This document addresses calculations of probability distribution functions (PDFs) representing uncertainties in projecting fatal cancer risk from galactic cosmic rays (GCR) and solar particle events (SPEs). PDFs are used to test the effectiveness of potential radiation shielding approaches. Monte-Carlo techniques are used to propagate uncertainties in risk coefficients determined from epidemiology data, dose and dose-rate reduction factors, quality factors, and physics models of radiation environments. Competing mortality risks and functional correlations in radiation quality factor uncertainties are treated in the calculations. The cancer risk uncertainty is about four-fold for lunar and Mars mission risk projections. For short-stay lunar missins (<180 d), SPEs present the most significant risk, but one effectively mitigated by shielding. For long-duration (>180 d) lunar or Mars missions, GCR risks may exceed radiation risk limits. While shielding materials are marginally effective in reducing GCR cancer risks because of the penetrating nature of GCR and secondary radiation produced in tissue by relativisitc particles, polyethylene or carbon composite shielding cannot be shown to significantly reduce risk compared to aluminum shielding. Therefore, improving our knowledge of space radiobiology to narrow uncertainties that lead to wide PDFs is the best approach to ensure radiation protection goals are met for space exploration.

14. SUBJECT TERMS

probability distribution functions; galactic cosmic rays; solar radiation; morality; radiation effects; radiation shielding; radiation; cancer; mission planning

15. NUMBER OF PAGES
44

16. PRICE CODE

17. SECURITY CLASSIFICATION OF REPORT	18. SECURITY CLASSIFICATION OF THIS PAGE	19. SECURITY CLASSIFICATION OF ABSTRACT	20. LIMITATION OF ABSTRACT
Unclassified	Unclassified	Unlimited	Unlimited